

# Transcriptome analysis of *CsWOX1* mutant and overexpressing lines reveals downstream genes regulating cucumber leaf morphogenesis

Anran Zhang , Xiangbao Li, Helong Zhang, Yanxin Jiang, Qingqing Li, Junjun Shen\* and Zheng Li\*

College of Horticulture, Northwest A&F University, Yangling 712100, Shaanxi, China

\* Corresponding authors, E-mail: [shenj@nwfau.edu.cn](mailto:shenj@nwfau.edu.cn); [lizheng82@nwsuaf.edu.cn](mailto:lizheng82@nwsuaf.edu.cn)

## Abstract

*WUSCHEL-related homeobox 1 (WOX1)*, categorized into the WUS clade, has been determined as the essential gene for leaf expansion as well as promoting leaf outgrowth along the mediolateral axis. The phenotypic characteristics of transgenic cucumber plants with *CsWOX1* overexpression (*CsWOX1*-OE) and mutants (designated as *mango fruit*, *mf*) have been reported. Specifically, *CsWOX1*-OE cucumber plants exhibit leaves with a distinctive 'butterfly-shaped' appearance, while *mf* mutants show a rapid reduction in the area of their leaf tips. In this study, RNA-Seq was employed to sequence the transcriptome of *CsWOX1*-OE to reveal its differentially expressed genes (DEGs). Combined with the transcriptome sequencing data of the *mf* mutant, GO classification, and KEGG pathway enrichment analyses were performed, revealing new links between the WOX1 protein and many core plant regulatory pathways. The further joint analysis identified 80 common DEGs between *CsWOX1*-OE and *mf*, with a significant proportion of these common DEGs being annotated to the circadian pathway and the auxin polarity transport pathway. Six genes (*CsGI*, *CsFKF1*, *CsRVE6*, *CsRVE8*, *CsABCB*, and *CsPin1At*) were selected for Y1H and Dual-LUC interaction validation experiments. These experiments demonstrated that *CsWOX1* directly targets the promoters of *CsRVE6*, which regulates leaf expansion, and *CsPin1At*, which is involved in auxin polarity transport, thereby promoting their transcription. In conclusion, these findings provide a foundation for exploring the potential regulatory mechanisms associated with *CsWOX1*, expecting to contribute to the construction of a more comprehensive gene network for leaf morphogenesis.

**Citation:** Zhang A, Li X, Zhang H, Jiang Y, Li Q, et al. 2025. Transcriptome analysis of *CsWOX1* mutant and overexpressing lines reveals downstream genes regulating cucumber leaf morphogenesis. *Vegetable Research* 5: e004 <https://doi.org/10.48130/vegres-0024-0038>

## Introduction

Shoot apical meristem (SAM), the origination of plant leaves, provides the stem cell niche to the whole of up-ground organs in higher plants, and has been divided into the central zone (CZ), renewing the meristem, as well as the peripheral zone (PZ) where the lateral organs emerge<sup>[1]</sup>. The process of leaf initiation and expansion depends on an elaborate and joint system. The regulatory networks for this procedure are constructed by various genes and transcription factors related to hormonal regulation, polarity establishment, and maintenance, as well as leaf flattening and expansion<sup>[2]</sup>. The initial cells of leaves derived from PZ grow along three asymmetric axes: proximal-distal axis, adaxial-abaxial axis, and mediolateral axis, and ultimately expand in multiple directions to a final leaf form<sup>[2–4]</sup>.

A gene expression pattern distinguishing adaxial and abaxial cells are established before leaf initiation<sup>[5,6]</sup>. The formation of the adaxial domain is promoted by the genes like *REVOLUTA (REV)*, *PHAVOLUTA (PHV)*, and *PHABULOSA (PHB)* containing the HD-ZIP III domain<sup>[7–10]</sup>, as well as *ASYMMETRIC LEAVES2 (AS2)* with a LOB-domain<sup>[11–13]</sup>. While *KANADI1 (KAN1)* promotes the initiation of the abaxial domain and this prepattern shifts dynamically during leaf development<sup>[6,14]</sup>.

In Arabidopsis, *REVILLE (RVE)* family genes negatively regulate leaf size. The *rve 4 6 8* mutant has enlarged mesophyll cells, and this gene family plays a crucial role in regulating the plant's biological clock<sup>[15,16]</sup>. The Arabidopsis *PIN1-type parvulin 1 (Pin1At)* gene is involved in auxin polar transport and the Pin1At protein influences PINOID (PID) and Protein Phosphatase 2A (PP2A)-mediated auxin transport and polar localization related to PIN-FORMED1 (PIN1) in the stele cells<sup>[17]</sup>. Additionally, overexpression of *Pin1At* in

Arabidopsis leads to serrated leaves and stems and accelerated flowering, indicating that the *Pin1At* gene regulates leaf morphogenesis and flowering time<sup>[18–20]</sup>.

The *WOX (WUSCHEL-related homeobox)* family comprises 15 members categorized into the WUS, Intermediate, and Ancient clades<sup>[21]</sup>. These members play critical roles in various aspects of plant growth and development, including the maintenance of meristematic stem cells, embryonic development, polarization, lateral organogenesis, and organ regeneration<sup>[22]</sup>. Specifically, WOX proteins are believed to define a central domain within the growing leaf bud. This domain acts as a separator between the abaxial and adaxial domains, controlling the outgrowth of the leaf blade. This function occurs downstream of the adaxial/abaxial polarity<sup>[23,24]</sup>.

In Arabidopsis, *WOX1*, *PRS*, and *WOX5* redundantly regulate the expression of the auxin biosynthesis gene *YUCCA (YUC)*, influencing regional growth along the leaf margin, thereby shaping the characteristic elliptical form of Arabidopsis leaves. Mutants lacking these genes exhibit narrower leaves<sup>[23,25]</sup>. Similar functions have been identified in various plant species, including *Nicotiana*, *Petunia*, *Medicago*, and garden pea<sup>[26–29]</sup>. The *WOX1* mutants in tobacco and tomato show significantly more severe leaf reduction, with almost no residual leaf tissue, and *WOX3* is unable to compensate for the loss of *WOX1* function<sup>[28,30]</sup>. Additionally, in tomato, *WOX1* not only plays a crucial role in leaf development but also regulates the initiation and growth of leaflets in compound leaves, indicating evolutionary diversity in *WOX1* function during compound leaf development<sup>[30]</sup>. In *Medicago truncatula*, the *WOX1* ortholog *STENO-FOLIA (STF)* primarily regulates leaf expansion, while the *WOX3* ortholog *LOOSE FLOWER (LFL)* primarily controls flower development, with minimal impact on leaf growth<sup>[31,32]</sup>. However, the expression patterns of monocots are different, like maize and rice

which control leaf blade outgrowth with *PR5* orthologs<sup>[33–35]</sup>. *WOX1* orthologs are expressed along the entire upper-lower leaf junction, while *PR5* orthologs have more restricted expression in the marginal meristem. These spatial differences in gene expression may explain variations in lateral leaf outgrowths between monocots and eudicots<sup>[33]</sup>. In the context of limited reporting on downstream genes associated with *WOX* genes, it is of paramount significance for the exploration of additional genes involved in leaf morphogenesis and the enrichment of downstream regulatory networks.

The leaf phenotypes of *CsWOX1* overexpressing and mutant cucumbers have been reported to show 'butterfly-shaped' leaves and a smaller blade horizontal-vertical ratio, especially in the distal region of the leaves<sup>[36,37]</sup>. Given the limited reporting on downstream genes related to *WOX* genes, the exploration of additional genes involved in leaf morphogenesis and the enhancement of downstream regulatory networks is of utmost importance. In this study, a transcriptomic analysis approach was utilized to obtain a significant dataset of differentially expressed genes. By comparing the differentially expressed genes between *CsWOX1*-overexpression (*CsWOX1*-OE) lines and mutants simultaneously, candidate downstream genes associated with the *CsWOX1* gene were identified.

## Materials and methods

### Plant materials and growth conditions

Cucumber (*Cucumis sativus* L.) inbred CU2 was selected as the wild type for comparison and cucumber genetic transformation. *CsWOX1*-OE were contemporary overexpression materials obtained through transgenic technology. Spontaneous mutant *mf* was identified from the cucumber line 'Extra Early Majestic', and sowing the seeds of *mf* and wild type (AM218).

Germinated seeds and transgenic plants with regenerative roots were transferred to seedling pots and cultivated in an artificial climate chamber. The chamber's temperature was maintained at 25 °C during the day and 20 °C at night, with a light/dark cycle of 16 h/8 h. Seedlings were transplanted into a sunlight greenhouse at the 4–6 true leaf stage. Fertilization, irrigation management, and pest and disease control were conducted following standard procedures.

### RNA isolation

RNA was extracted from 1 cm-long apical leaves at the early expansion stage, selected from 30-day-old *CsWOX1*-OE transgenic lines, *mf* mutants, and wild-type plants (CU2 and AM218). Three biological replicates were performed for each genotype sample, and the extracted RNA was used for RNA-Seq and RT-qPCR analysis. For each sample, the leaves were immersed in liquid nitrogen within a mortar and ground into a fine powder. Total RNA was extracted using kit (TIANGEN, China). The integrity and quality of the total RNA were assessed using a NanoDrop 1000 spectrophotometer and formaldehyde-agarose gel electrophoresis.

### Transcriptome analysis

Six samples from *CsWOX1*-OE and CU2 were submitted to Bio-Marker Biomarker Technology (Beijing, China) for RNA sequencing. After verifying the purity, concentration, and integrity of the RNA samples, cDNA library construction and quality inspection were carried out. PE150 mode sequencing was performed utilizing the Illumina NovaSeq6000 sequencing platform. Clean data with high quality was obtained by filtering raw data, which removes adapter sequences and reads with low quality. Clean reads were aligned with the reference genome (*Cucumis sativus*. ChineseLong\_v3. genome. fa) through HISAT2 software and the reads were compared on the pair for assembly by StringTie software. After obtaining Mapped Data, library quality evaluation, variable splicing analysis,

gene structure optimization, differential expression analysis, gene functional annotation, and functional enrichment were performed. Data normalization was achieved through Reads Per Kilobase of transcript, per Million mapped reads (RPKM). Differential expression genes were screened by DESeq2 software, with Fold Change (FC)  $\geq 2$  and False Discovery Rate (FDR)  $< 0.01$  as the screening criteria.

### RT-qPCR

To assess the fidelity of the RNA-seq data, six genes exhibiting opposite expression patterns between *CsWOX1*-OE and *mf* were chosen for RT-qPCR analysis. The first-strand cDNA was synthesized *via* reverse transcription of the total RNA extracted, employing the HiScript II 1st Strand cDNA Synthesis Kit following the manufacturer's guidelines (Vazyme, China). Subsequently, RT-qPCR was conducted using the SYBR qPCR Master Mix (Vazyme, China) on an ABI 7500 Fast Real-Time PCR System (Applied Biosystems, USA). Each gene was subjected to three biological and three technical replicates. The resulting relative expression data were normalized against the expression level of the cucumber *CsActin2* gene<sup>[38]</sup>. The  $2^{-\Delta\Delta Ct}$  method<sup>[39]</sup> was employed for calculating the relative expression levels of each gene. The primer sequences are provided in [Supplementary Table S1](#).

### Yeast one-hybrid assay

*CsWOX1* coding sequences were cloned into the pB42AD plasmid. Subsequently, the promoter fragment of approximately 2.0-kb from *CsRVE6*, *CsRVE8*, *CsABC6*, and *CsPin1A1* were cloned into the pLacZi2u plasmid. The primer sequences are detailed in [Supplementary Table S1](#). Following this, the pB42AD-*CsWOX1* and pLacZi2u-*pCsRVE6/pLacZi2u-pCsRVE8/pLacZi2u-pCsABC6/pLacZi2u-pCsPin1A1* constructs were co-transformed into the yeast EGY48 strain and cultured at 30 °C for 2–4 d on SD/-Trp/-Ura plates. Monoclonal yeast transformants were selected and cultured on SD/-Trp/-Ura/X-gal plates for 2–4 d to ascertain protein-protein interactions. The observation of both normal colony growth and the development of a blue coloration indicates the plausible occurrence of mutual interactions between the two proteins.

### Dual-luciferase reporter assay

A 952 bp sequence located upstream of the translation initiation start site of *CsRVE6* was integrated into the transient expression vector, pGreenII 0800-Luc, thereby generating a Pro*CsRVE6*: *LUC* reporter construct. Subsequently, the CDS sequence of *CsWOX1* were inserted into pGreenII 62-SK, resulting in the creation of 35S:*CsWOX1* effectors. The reporter and effectors were independently transformed into GV3101-pSoup. For each effector, a transient co-infiltration was conducted into *N. benthamiana* leaves alongside the pGreenII 62-SK vector and Pro*CsRVE6*:*LUC* reporter serving as a negative control, maintaining an effector : reporter ratio of 9:1<sup>[40]</sup>. Each experimental condition encompassed three biological replicates and three technical replicates, followed by the execution of the dual-luciferase reporter assay<sup>[36]</sup>. The activities of firefly luciferase (*LUC*) and Renilla luciferase (*REN*) were quantified using a Dual-Luciferase reporter gene detection kit (Yeasen Biotech, Shanghai, China), adhering to the manufacturer's instructions. The primer sequences utilized are provided in [Supplementary Table S1](#).

## Results

### Sequencing and transcriptome analysis of *CsWOX1*-OE

To elucidate the downstream regulatory network of *CsWOX1* gene and identify potential candidate genes related to leaf morphogenesis, transcriptome analysis was performed on *CsWOX1*-OE

transgenic lines and wild-type CU2 utilizing RNA-Seq. Six samples, divided into two groups with three biological replicates each, were processed for transcriptome sequencing, generating 47.09 Gb of clean data. At least 6.80 Gb clean data were generated for each sample with a minimum 93.67% of clean data achieving a quality score of Q30 (Supplementary Table S2). Clean reads of each sample were mapped to the specified reference genome. The mapping ratio ranged from 95.38% to 97.56% (Supplementary Table S3).

Principal Component Analysis (PCA) based on the transcriptome data from *CsWOX1*-OE and the wild type (CU2) revealed clear separation between the two groups, highlighting significant differences. The proximity of biological replicates within each group indicated similar sample compositions with minimal variations (Fig. 1a). Between *CsWOX1*-OE and the wild type, a total of 3,757 differentially expressed genes (DEGs) were identified, comprising 2,517 upregulated and 1,240 downregulated genes (Fig. 1b). All the DEGs were functionally annotated in eight databases: COG, GO, KEGG, KOG, NR, Pfam, Swiss-Prot, and eggNOG. The number and percentage of DEGs annotated in each database are shown in Fig. 1c. Prediction of alternative splicing, gene structure optimization analysis and novel gene discovery was processed on top of mapping results, during which 955 were discovered and 422 novel genes were annotated with a putative function.

### Combined analysis of *CsWOX1*-OE and *mf* transcriptome sequencing results

Based on the published RNA-Seq data of *mf*<sup>[37]</sup>, a combined analysis of the transcriptome data from the *CsWOX1*-OE and the mutant

was conducted. Compared with the 3,757 DEGs found in *CsWOX1*-OE, only 200 DEGs were found in the RNA-Seq results of *mf*, with 59 upregulated genes and 141 downregulated genes<sup>[37]</sup>.

The DEGs of *CsWOX1*-OE and *mf* were analyzed by Gene Ontology (GO), and the GO classification was divided into three main categories: biological process (BP), cellular component (CC), and molecular function (MF). The results, as shown in Fig. 2, showed that in *CsWOX1*-OE and *mf*, cellular and cellular fractions accounted for the largest proportion of cellular components, with 1,643 and 95 DEGs annotated, respectively. Binding and catalytic activities were the two most dominant molecular functions of DEGs. Cell process, metabolic process, and single-organism process were the biological processes with the highest number of defined DEGs. In addition, KEGG pathway enrichment analysis was performed on the DEGs of *CsWOX1*-OE and *mf*. This analysis revealed the impact of the *CsWOX1* gene on various biological processes and metabolic pathways in cucumber (Fig. 3). The pathways annotated with DEGs were classified into five categories: Cellular Processes, Environmental Information Processing, Genetic Information Processing, Metabolism, and Organismal Systems, among which the metabolic pathways annotated the largest number of DEGs, both in *CsWOX1*-OE and *mf*. In *mf*, the pathway with the most DEGs was the starch and sucrose metabolic pathway, which accounted for 13.64% of all DEGs. In *CsWOX1*-OE, the plant-pathogen interaction pathway and the plant hormone signaling pathway annotated the first and second place with 9.88% of 140 DEGs and 8.82% of 125 DEGs, respectively. This indicates that the elevated expression level of *CsWOX1* expression significantly affects plant disease resistance and hormone signal mechanisms.

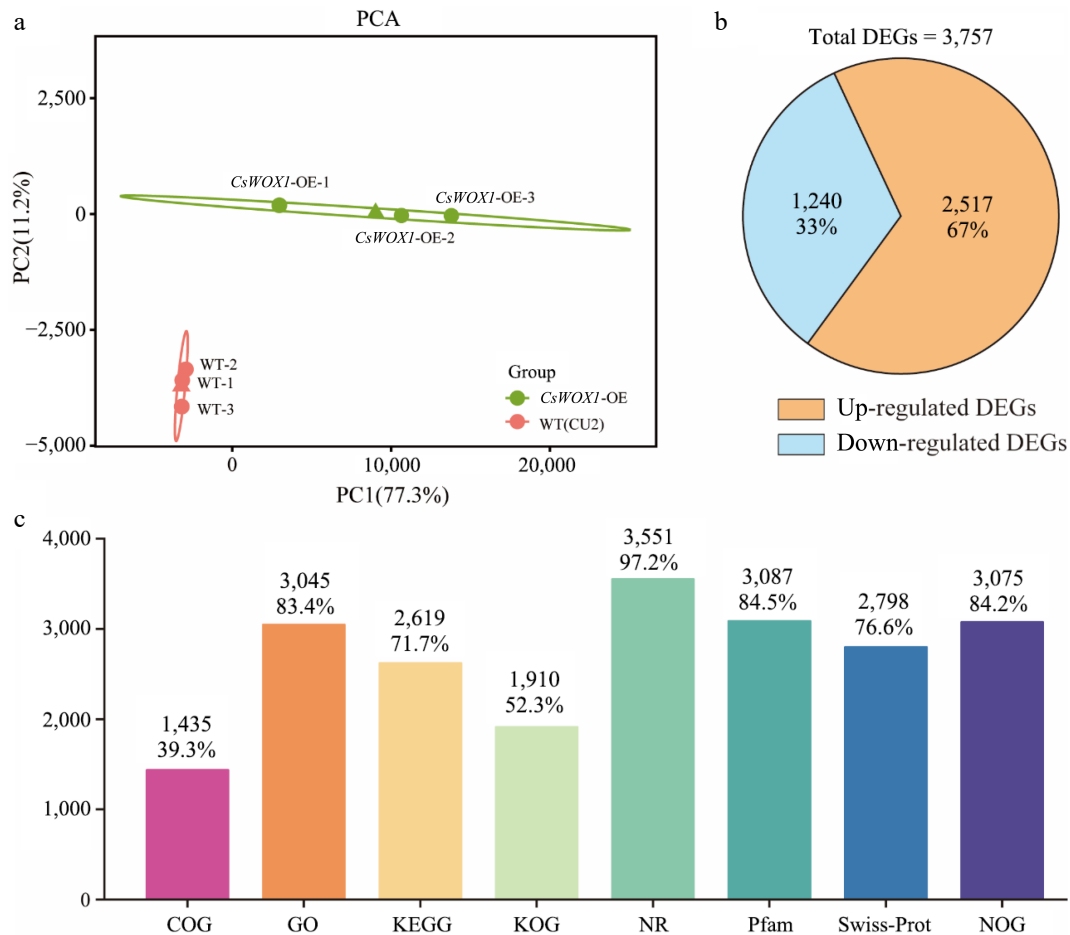


**Fig. 1** Transcriptome information and analysis of *CsWOX1*-OE. (a) The principal component analysis (PCA) of differentially expressed transcripts from two groups. (b) Statistics on the number of up-regulated and down-regulated DEGs. (c) The number and proportion of DEGs annotated in different databases.

Through joint comparative analysis, we found that there were 80 identical genes in the DEGs of *CsWOX1*-OE and *mf*, called common DEGs (Fig. 4a). By analyzing the changes in the expression trends of these 80 common DEGs, it was found that 20 of these genes showed the same change trends in *CsWOX1*-OE and *mf*, either increasing or decreasing together, while the other 60 genes showed opposite expression changes. The expression levels of these 20 DEGs with the same trend and 60 DEGs with opposite trends in *CsWOX1*-OE and *mf* were shown in Fig. 4b and c, respectively, and the heatmaps were plotted by the  $\log_2$  FC values of the DEGs. Since *CsWOX1* expression was opposite in *CsWOX1*-OE and *mf*, this study focusses on the 60 common DEGs with opposite changes in expression trends. The KEGG pathway analysis revealed that these 60 common DEGs were annotated into 26 pathways, of which three pathways, namely, circadian-plant (ko04712), MAPK signaling pathway-plant (ko04016), and plant-pathogen interaction (ko04626), all three pathways were enriched with more than two common DEGs (Table 1).

### Validation of differentially expressed genes

To verify the accuracy of Illumina sequencing data, six common DEGs with opposite expression trends in *CsWOX1*-OE and *mf* were selected for RT-qPCR to detect their expression changes. Four genes involved in the plant circadian pathway were selected, *GIGANTEA* (*CsGI*, *CsaV3\_7G024490*), *FLAVIN-BINDING KELCH REPEAT F-BOX 1* (*CsFKF1*, *CsaV3\_5G014370*), *REVILLE6* (*CsRVE6*, *CsaV3\_3G017490*), and *REVILLE8* (*CsRVE8*, *CsaV3\_3G035450*), as well as two genes involved in growth hormone transport, *ATP BINDING CASSETTE subfamily B* (*CsABCB*, *CsaV3\_5G029720*), and *Arabidopsis PIN1-type parvulin 1* (*CsPin1At*, *CsaV3\_4G005720*).

The relative expression levels of these six genes in the wild type, *CsWOX1*-OE, and *mf* are shown in Fig. 5. The relative expression levels of the genes were calculated by the  $2^{-\Delta\Delta CT}$  method and analyzed for significant differences, which showed that the expression level of the *CsRVE8* gene was significantly decreased in *CsWOX1*-OE and significantly increased in *mf*. In contrast, the expression levels of the other five genes were significantly increased in *CsWOX1*-OE and significantly decreased in *mf*. Although the fold change of genes differed between the transcriptome data and the RT-qPCR results due to the sensitivity of the different techniques, the trends in the expression levels of the six genes detected by RT-qPCR were consistent with the RNA-Seq results, which proved that the data from RNA-Seq were accurate and reliable.

### CsWOX1 regulates auxin polar transport-related genes

Previous studies have shown significant changes in leaf size and shape in *CsWOX1*-OE and *mf* that are associated with the polarity transport of auxin and the response to auxin polarity signaling<sup>[36,37,41]</sup>. By analyzing the KEGG pathway in *mf* and *CsWOX1*-OE, it was found that many DEGs have been annotated to the phytohormone signaling pathway (ko04075) and most of the DEGs involved in the auxin transduction showed up-regulation. AUXIN RESISTANT1 (AUX1, K13946), auxin influx carrier, expressed increasingly both in *CsWOX1*-OE and *mf*, which were regulated by *CsaV3\_3G034000* and *CsaV3\_2G015870*, respectively. The upregulated gene in *mf* (*CsaV3\_2G013720*) affected the regulation of the auxin-responsive protein IAA: AUX/IAA (K14484), which was jointly controlled by four upregulated genes (*CsaV3\_2G004120*, *CsaV3\_*

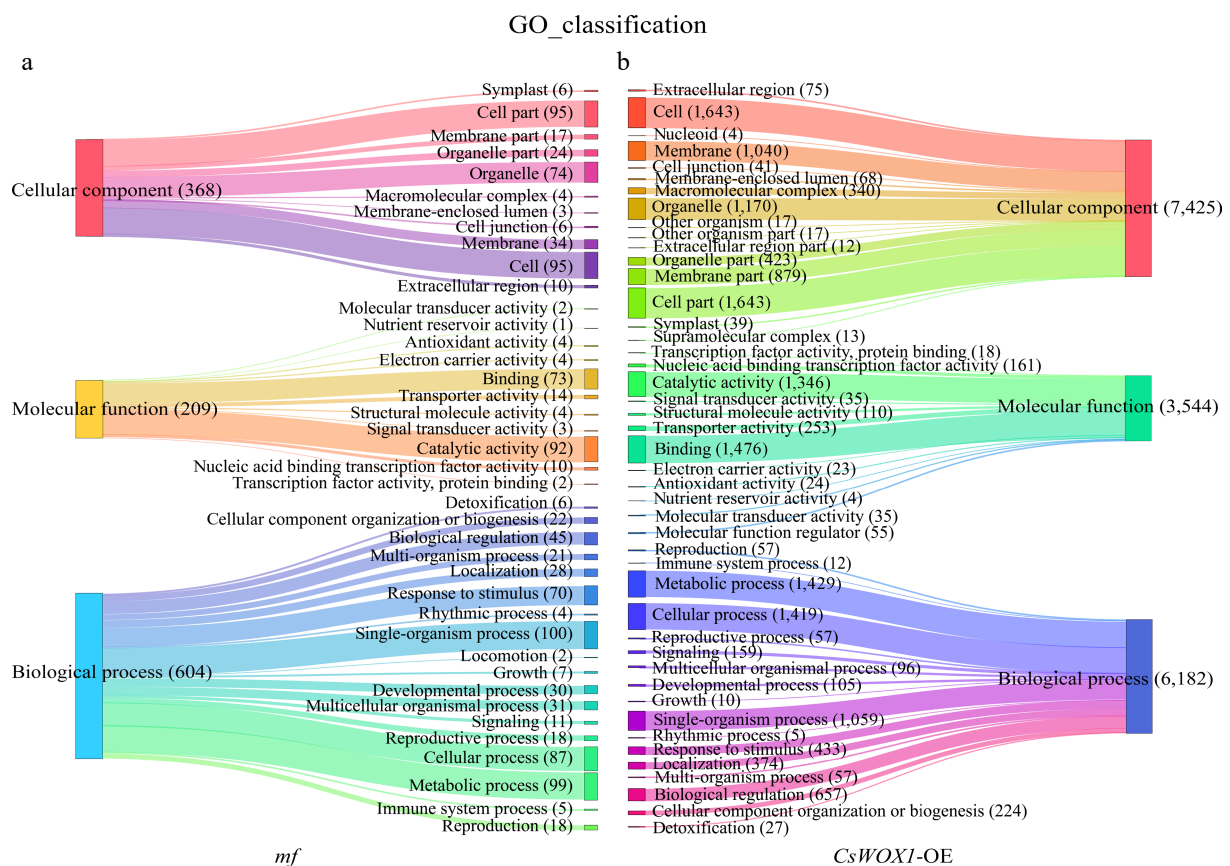


**Fig. 2** The GO classification analysis results show the differences in the number and categories of annotated DEGs between the *mf* and *CsWOX1*-OE, with three main GO categories: Cellular component, Molecular function, and Biological process. (a) GO classification of DEGs in the *mf* sample. (b) GO classification of DEGs in the *CsWOX1*-OE sample. Each band represents the annotation status and trends of different GO terms and the numbers in parentheses indicate the number of genes in each category.

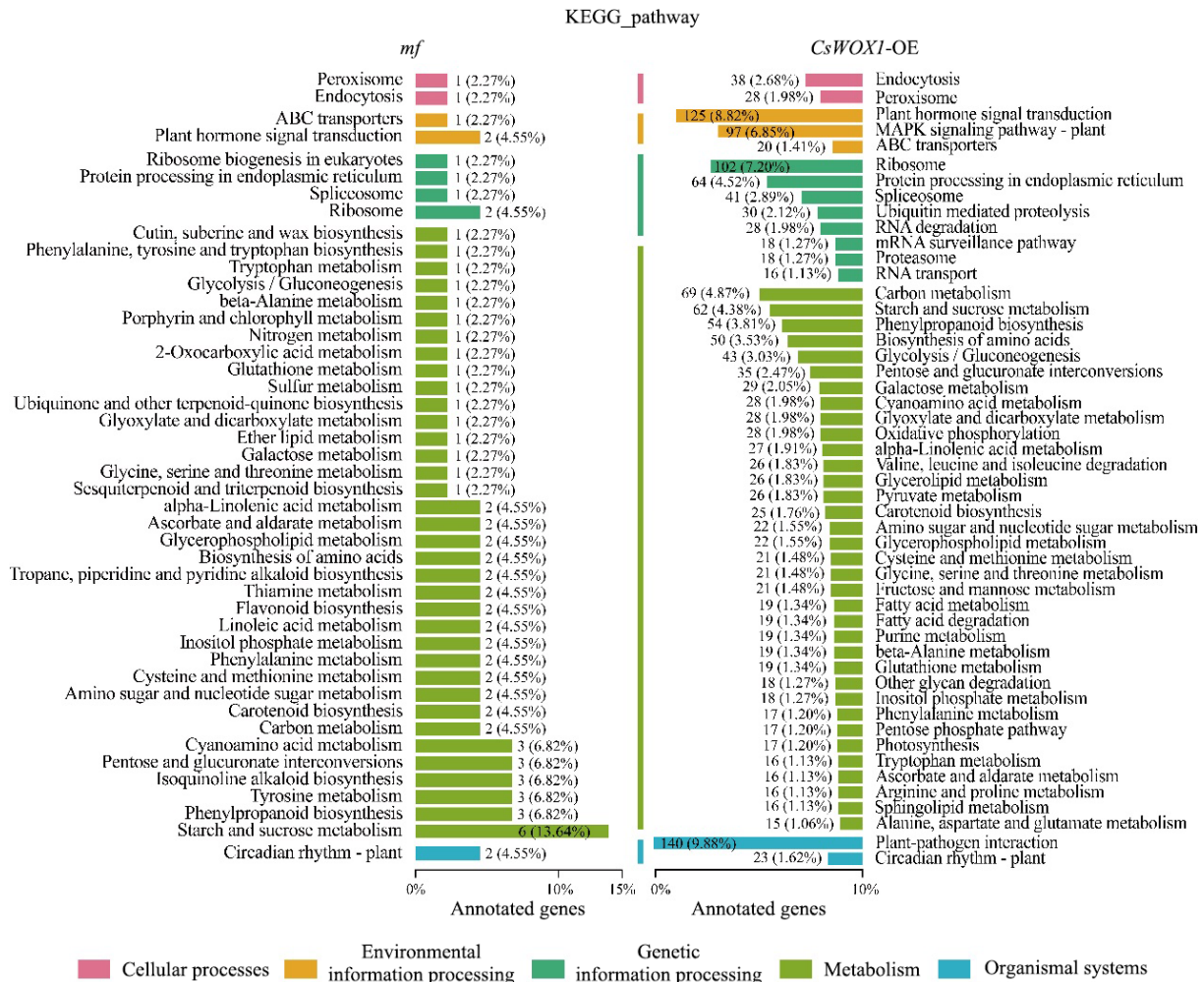


**Fig. 3** KEGG pathway analysis of the DEGs from *mf* and *CsWOX1*-OE shows the number and proportion of DEGs annotated in different metabolic pathways. The KEGG pathways are categorized into five groups: cellular processes, environmental information processing, genetic information processing, metabolism, and organismal systems.

2G013230, *CsaV3\_3G023550*, and *CsaV3\_3G048770*) and one down-regulated gene (*CsaV3\_3G012650*) in *CsWOX1*-OE. As for the AUXIN RESPONSE FACTOR (ARF, K14486), it was only upregulated in *CsWOX1*-OE, regulated by *CsaV3\_1G023020* and *CsaV3\_6G036480*.

Joint analysis of the DEGs involved in the polarity transport of auxin were conducted, identifying two common DEGs: the homologs genes of the *ABCB* and *Pin1At*. The *ABCB* encodes phosphoglycol proteins (PGP), and they have been shown to participate in plant auxin efflux by stabilizing PIN proteins in the plasma membrane<sup>[42,43]</sup>. In *CsWOX1*-OE transgenic lines, the expression of the *CsABCB* gene increased by 2.71 times and its expression level was reduced by 2.07 times in mutants. *Pin1At*, peptidyl-prolyl cis/trans isomerase gene<sup>[20]</sup>, affects PIN1-related auxin transport and polarity localization in mesocolumnar cells mediated by PID and PP2A as well as catalyzes the conformational change of the phosphorylated Ser/Thr-Pro motif in PIN1<sup>[17]</sup>. *CsPin1At* exhibited up-regulation in *CsWOX1*-OE transgenic lines and down-regulation in *mf* mutants.

Both of these genes exhibited a consistent expression pattern, with an upregulation in the *CsWOX1*-OE and a downregulation in the *mf*. This result suggests a correlation between the *CsWOX1* gene and auxin transport and distribution, which could potentially influence leaf development.

### **CsWOX1 regulates the genes controlling plant rhythms and leaf expansion**

In *CsWOX1*-OE, plenty of core circadian clock-related genes annotated in rhythm pathways expressed differently from the wild type, such as the upregulated genes: *Early Flowering 3 (ELF3)*, *Phytochrome-Interacting Factor 3 (PIF3)*, *PSEUDO-RESPONSE REGULATOR 5 (PRR5)*, and *PSEUDO-RESPONSE REGULATOR 7 (PRR7)*. As for the LATE ELONGATED HYPOCOTYL (LHY) transcription factor with an MYB-like domain, its homologous gene *RVE6* was upregulated while *RVE8* was downregulated. Furthermore, the expression of *CRYPTOCHROME (CRY)*, which receives blue light signals, was increased, and the expression of *CONSTITUTIVE PHOTOMORPHOGENIC 1 (COP1)*, which is inhibited by *CRY*, decreased. The expression of *GI*, *FKF1*, *CYCLING DOF FACTOR 1 (CDF1)*, and *CONSTANS (CO)* all increased, and they collectively regulate plant flowering.

In the plant circadian rhythm regulation pathway, only *GI*, *FKF1*, *RVE6*, and *RVE8* are co-DEGs, and their trends of expression change showed exactly opposite directions in *CsWOX1*-OE and *mf*. *GI* and *FKF1* participate in the blue light signal transduction pathway and the regulation of photoperiod flowering<sup>[44,45]</sup>. *RVE6* and *RVE8* have been determined to promote clock pace in a partially redundant manner with their homologs *REVILLE4*, as well as control leaf surface area and cell size, resulting in a 30% increase in the average area of

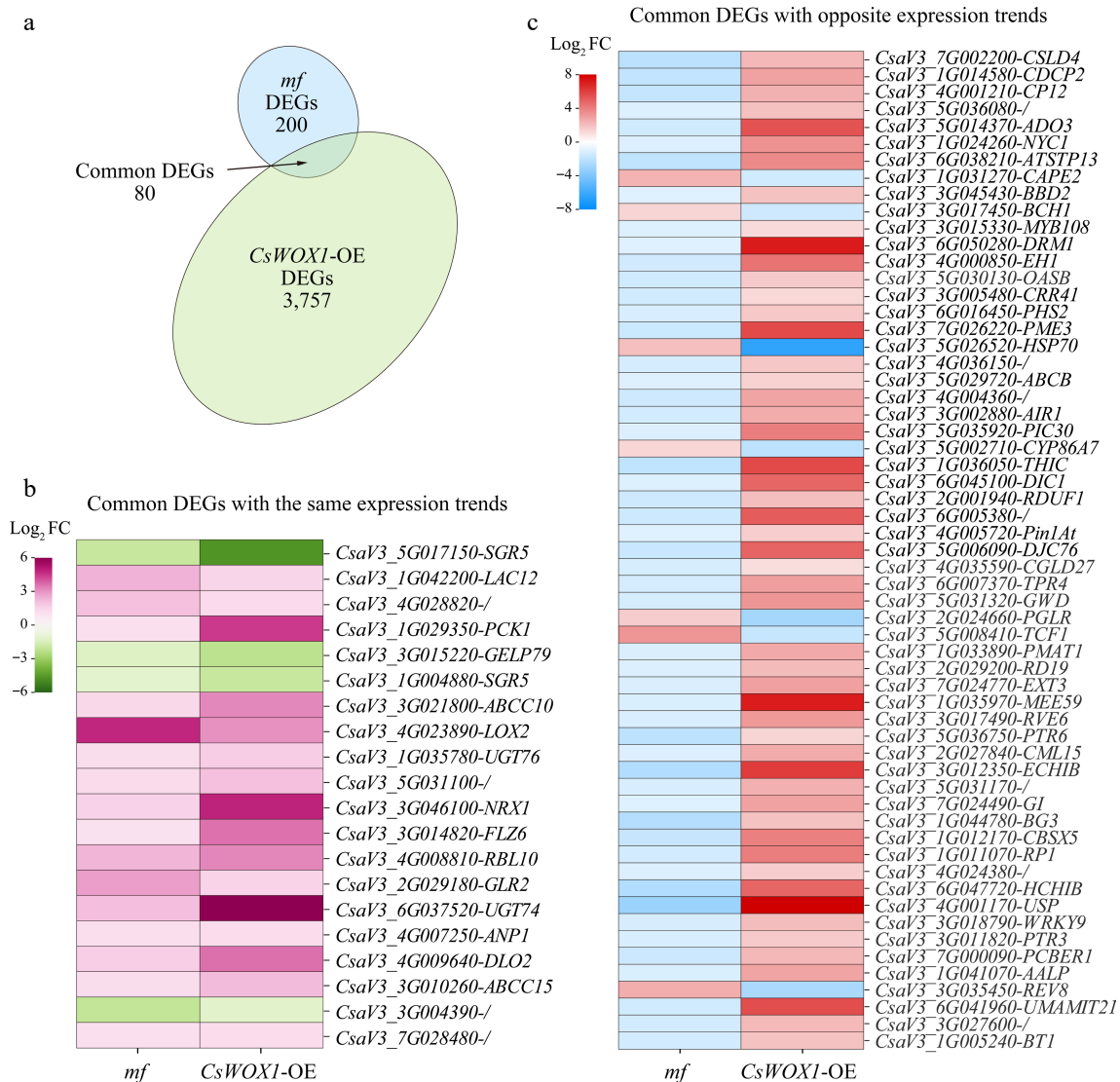


**Fig. 4** Combined analysis of *mf* and *CsWOX1*-OE DEGs. (a) Identification of eight common DEGs between *mf* and *CsWOX1*-OE. (b) Heatmap of gene expression levels of 20 common DEGs with the same trend of change. (c) Heatmap of gene expression levels of 60 common DEGs with opposite trends. The colored legend positioned to the left of each map indicates fold changes ( $\text{Log}_2$  value).

mesophyll cells in the *rve4 rve6 rve8* mutant<sup>[15]</sup>. The relative expression changes of the homologous genes *CsRVE6* and *CsRVE8* in *CsWOX1*-OE and *mf* not only exhibit opposite trends but also have a complementary relationship. Specifically, when *CsRVE6* expression increased in *CsWOX1*-OE, *CsRVE8* expression decreased; in *mf*, when *CsRVE6* was downregulated *CsRVE8* was then upregulated.

A large number of DEGs were identified in the plant circadian regulatory pathway and there were four co-DEGs, of which *CsRVE6* and *CsRVE8* were associated with the formation of leaf surface area. This provides a basis for the involvement of the *CsWOX1* gene in plant circadian regulation and establishes a new link between rhythm-related genes and leaf development.

### CsWOX1 binds and transcriptionally activates the promoter of *CsRVE6* and *CsPin1At*

Through comparative analysis of the transcriptomic data between *CsWOX1* overexpression and *mf*, significant changes in the expression levels of genes involved in auxin polar transport and plant circadian rhythm regulation were found. To test whether *CsWOX1* directly binds to the promoters of six common DEGs (*CsRVE6*, *CsRVE8*, *CsGI*, *CsFKF1*, *CsPin1At*, and *CsABCB*), yeast one-hybrid

experiments were conducted with the promoter sequences (about 2,000 bp) of these genes and the *CsWOX1* transcription factor. The results indicated that the *CsWOX1* transcription factor binds only to the promoters of *CsRVE6* and *CsPin1At*, causing the corresponding yeast colonies to turn blue in SD/-Ura/-Trp/X-gal medium (Fig. 6). Regarding the remaining four genes, they didn't exhibit transcriptional regulation by *CsWOX1* transcription factor.

A dual-LUC reporter assay was employed to examine the impact of *CsWOX1* on the activity of the firefly luciferase gene (LUC) driven by the promoters of *CsPin1At* or *CsRVE6* in *N. benthamiana* leaves. The co-expression of 35S:*CsWOX1* with *proCsPin1At:LUC* or *proCsRVE6:LUC* vectors resulted in a significant increase in LUC/REN signals of approximately 15-fold and 5-fold, respectively, compared to expression of *proCsPin1At:LUC* or *proCsRVE6:LUC* vectors alone (Fig. 7). This observation suggests that the *CsWOX1* transcription factor activates the expression of *CsPin1At* and *CsRVE6*.

To elucidate the expression patterns of *CsRVE6* and *CsPin1At*, an analysis of their gene expression in various cucumber organs was conducted, including the root, stem, leaf, petal, sepal, tendril, and apical bud, using RT-qPCR (Supplementary Fig. S1). The results revealed that *CsRVE6* is predominantly expressed in the petal, sepal,

**Table 1.** Joint KEGG pathway analysis of common DEGs in CsWOX1-OE and *mf*.

Pathway ID	Pathway name	Common DEGs
ko00906	Carotenoid biosynthesis	CsaV3_1G014580, CsaV3_3G017450
ko04712	Circadian rhythm - plant	CsaV3_5G014370, CsaV3_3G017490, CsaV3_7G024490, CsaV3_3G035450
ko00860	Porphyrin and chlorophyll metabolism	CsaV3_1G024260
ko04016	MAPK signaling pathway - plant	CsaV3_1G031270, CsaV3_6G047720, CsaV3_3G018790
ko04075	Plant hormone signal transduction	CsaV3_1G031270
ko04626	Plant-pathogen interaction	CsaV3_1G031270, CsaV3_2G029200, CsaV3_2G027840, CsaV3_3G018790
ko00590	Arachidonic acid metabolism	CsaV3_4G000850
ko04146	Peroxisome	CsaV3_4G000850
ko00270	Cysteine and methionine metabolism	CsaV3_5G030130
ko00920	Sulfur metabolism	CsaV3_5G030130
ko01200	Carbon metabolism	CsaV3_5G030130
ko01230	Biosynthesis of amino acids	CsaV3_5G030130
ko00500	Starch and sucrose metabolism	CsaV3_6G016450, CsaV3_1G044780
ko00040	Pentose and glucuronate interconversions	CsaV3_7G026220, CsaV3_2G024660
ko03040	Spliceosome	CsaV3_5G026520
ko04141	Protein processing in endoplasmic reticulum	CsaV3_5G026520
ko04144	Endocytosis	CsaV3_5G026520, CsaV3_7G024770
ko02010	ABC transporters	CsaV3_5G029720
ko00073	Cutin, suberine and wax biosynthesis	CsaV3_5G002710
ko00730	Thiamine metabolism	CsaV3_1G036050
ko04120	Ubiquitin mediated proteolysis	CsaV3_5G008410
ko00943	Isoflavonoid biosynthesis	CsaV3_1G033890
ko00944	Flavone and flavonol biosynthesis	CsaV3_1G033890
ko00071	Fatty acid degradation	CsaV3_3G012350
ko03008	Ribosome biogenesis in eukaryotes	CsaV3_5G031170
ko00520	Amino sugar and nucleotide sugar metabolism	CsaV3_6G047720

tendrils, apical bud, and leaf, whereas *CsPin1At* exhibits high expression in the petal, sepal, tendril, and root. These differential expression patterns hint at the potential functions of *CsRVE6* and *CsPin1At* in diverse cucumber organs, offering valuable insights for future research into their specific contributions to plant development.

## Discussion

In the present investigation, RNA-seq technology was employed to identify downstream DEGs of *CsWOX1*-OE and joint analysis performed with transcriptome sequencing results of the mutant *mf*. The RNA-Seq dataset substantially augmented our comprehension of the regulatory network involving *CsWOX1* by furnishing a comprehensive collection of differentially expressed genes. This enriched our insight into the involvement of *WOX1* in diverse growth and developmental pathways in cucumber. Given the substantial number of DEGs and the objective of pinpointing downstream genes intricately linked to *CsWOX1* expression variations, a cross-analysis of the 3,657 DEGs in *CsWOX1*-OE and the 200 DEGs in *mf* was conducted, identifying 80 common DEGs. Subsequently, an in-depth analysis was performed to unravel the profound implications of the *WOX1* gene in organ development, hormonal regulation, and various facets of plant growth and development pathways. Utilizing a comprehensive analytical approach encompassing GO,

KEGG pathway analysis, gene expression trends, and RT-qPCR, six differentially expressed genes were identified as potential candidate genes.

Initially, it is noteworthy that both *CsWOX1*-OE and mutant cucumbers demonstrated significant alterations in leaf morphology. The *mf* displayed a marked reduction in the leaf tip area and an acicular constriction on either side of the leaf veins, whereas the over-expressing plants displayed a butterfly-like leaf structure. Consequently, investigating the expression changes of the *ABCB* and *Pin1At* genes became the focus of the study.

Through homology analysis, it was identified that *CsaV3\_5G029720* shares the highest homology with *AtABCB21* in Cluster II of the *ABCB* subfamily in *Arabidopsis*<sup>[46]</sup>. It has been established that *ABCB21* plays a pivotal role in controlling auxin concentration in plant cells, serving as a conditional input/output transporter. Specifically, when the cytoplasmic IAA concentration is low, *ABCB21* mediates the inward transport of auxin, whereas in cases of high cytoplasmic IAA concentration, *ABCB21* facilitates outward auxin transport<sup>[46]</sup>. Notably, during the developmental stage of 7–10 d in *Arabidopsis* seedlings, *ABCB21* exhibits specific expression on the abaxial side of cotyledons and in the root region<sup>[46,47]</sup>, concomitant with the expression of *WOX1* in these same areas<sup>[41]</sup>. Furthermore, *ABCB21* has been implicated in the lateral distribution of auxin in *Arabidopsis* leaf blades. When *abcb21-1* (a weak allele of *ABCB21*) is further mutated on the background of *abcb1 abcb19* mutants, the resulting phenotype shows reduced leaf length and smaller epidermal cells<sup>[47–49]</sup>, consistent with the reduced leaf cell size observed in *mf* mutant plants<sup>[23,41]</sup>. These observations lead us to speculate that in cucumber, although the *WOX1* gene does not directly interact with *ABCB*, it may still affect auxin transport and regulate plant leaf cell growth and expansion.

The *Pin1At* gene has been shown to control the floral transition in plants by accelerating the cis/trans isomerization of phosphorylated Ser/Thr-Pro motifs in two MADS-box transcription factors<sup>[18,19]</sup>, SUPPRESSOR OF OVEREXPRESSION OF CO 1 (SOC1), and AGAMOUS-LIKE 24 (AGL24)<sup>[17,20]</sup>. Overexpression of *Pin1At* in *Arabidopsis* leads to an expedited flowering process, accompanied by the emergence of serrated leaves and cauline leaves<sup>[20]</sup>, indicating that *Pin1At* influences flowering time and leaf morphology in plants. Additionally, *CsPin1At* exhibits higher expression levels in petals, sepals, lateral branches, and roots, which may be related to the development of floral organs, lateral meristems, and root apical meristems.

Additionally, yeast one-hybrid assay indicated that the *LHY* homologous gene, *CsRVE6*, was transcriptionally activated by *CsWOX1*, whereas *CsRVE8* was not. *RVE6* and *RVE8* transcription factors are homologous to CIRCADIAN CLOCK ASSOCIATED1 (CCA1) and *LHY*<sup>[50,51]</sup>. CCA1 and *LHY* are homologous transcription factors with MYB-like domains and play pivotal roles in the plant circadian clock<sup>[52,53]</sup>. CCA1 and *LHY* suppress the expression of *TIMING OF CAB EXPRESSION1* (*TOC1*), forming a negative feedback regulation loop<sup>[54,55]</sup>. CCA1 and *LHY* inhibit *TOC1* expression, and *TOC1*, in turn, inhibits the expression of CCA1, *LHY*, and other genes from the *PRR* family<sup>[56–58]</sup>. *RVE8*, on the other hand forms an additional feedback loop within the circadian clock. *RVE8* positively regulates *PRR5*, and *PRR5* protein, in turn, suppresses the expression of *RVE8*<sup>[16,50,51]</sup>.

In *Arabidopsis*, the *RVEs* partially redundantly promote the circadian rhythms<sup>[16]</sup> and negatively regulate leaf cell growth rate and expansion area<sup>[15,16]</sup>. The leaves of adult triple *rve* mutants (*rve 4 6 8*) and quintuple *rve* mutants (*rve 3 4 5 6 8*) are approximately 30% larger than those of wild-type *Arabidopsis*, and this change is attributed to a 30% increase in cell area in leaves of the same age. Further research suggests that the *RVE* gene family negatively regulates plant responses to sucrose at concentrations ranging from

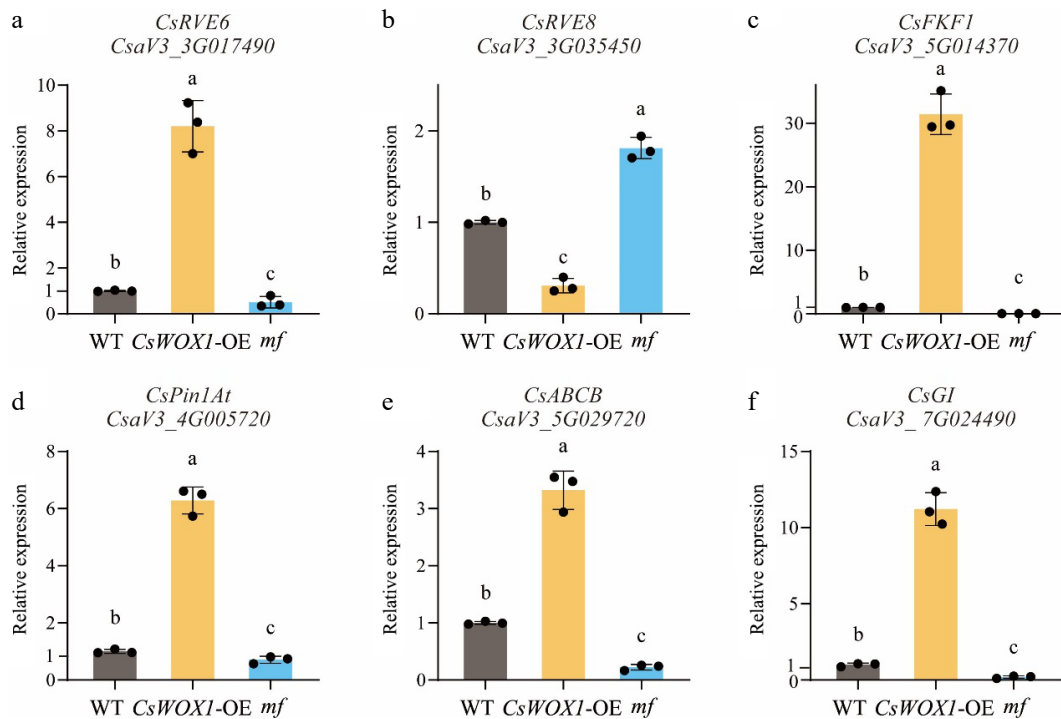


**Fig. 5** RT-qPCR analyses of (a) *CsRVE6*, (b) *CsRVE8*, (c) *CsFKF1*, (d) *CsPin1At*, (e) *CsABCB*, and (f) *CsGI* in *CsWOX1*-OE and *mf*. Significance analyses compared to WT were performed with the two-tailed Student's t-test. Different letters (a, b, c) indicate significant differences between groups ( $p < 0.05$ ). The values represent the mean  $\pm$  SD ( $n = 3$ ).

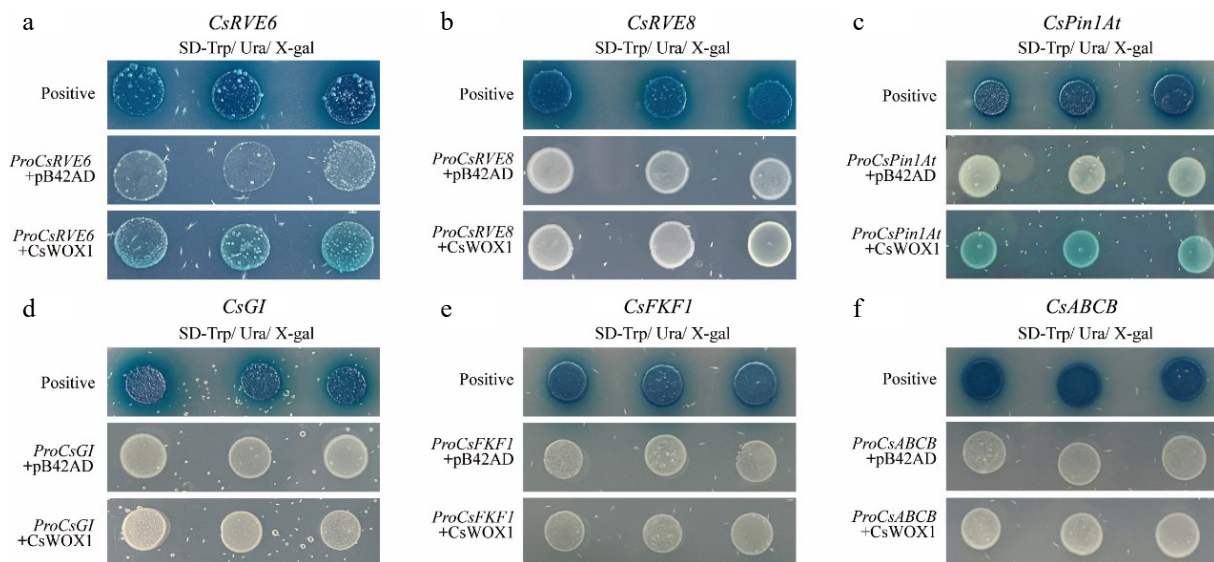


**Fig. 6** Yeast-one hybrid validation between *CsWOX1* transcription factors and candidate genes, which showed that *CsWOX1* bound to the promoters of *CsRVE6* and *CsPin1At*.

0.5% to 6%<sup>[15,59]</sup>. This, to some extent, explains the phenomenon of increased leaf area in *rve* multiple mutants. In cucumber, *CsRVE6* is highly expressed in petal and sepal, tendril, apical bud, and leaf, suggesting *CsRVE6* may play a critical role in the growth and development of these tissues, particularly in flower development and the growth of lateral branches and shoot apices.

Moreover, the *rve* multiple mutants exhibit a delay in flowering time<sup>[15]</sup>. Notably, the transition from vegetative to reproductive growth in plants is intricately linked, with photoperiodic rhythms governed by the circadian clock playing a crucial role in this process<sup>[60]</sup>. Under long-day conditions, the precise regulation of CO protein expression is pivotal for inducing flowering<sup>[61,62]</sup>. Previous

studies have elucidated that *FKF1* contributes to the stabilization of CO protein expression through two distinct pathways: one involving *FKF1* itself, and the other involving *CDF1*, which cooperates with *GI* to alleviate the inhibition on CO and FT transcription<sup>[63,64]</sup>.

Noteworthy is the observation that within the entire flowering regulation pathway, spanning from the light-sensitive *CRY*, through *ELF3*, *GI*, *FKF1*, *CDF1*, and *CO* genes, all of them, except for *COP1*, exhibited upregulated expression in *CsWOX1*-OE plants. As *CsWOX1* expression increased, the genes that inhibit *CDF1* also exhibited an upregulation in expression, resulting in an upregulation of *CDF1* expression. This may be a regulatory mechanism through which the plant seeks to maintain equilibrium in flowering regulation.

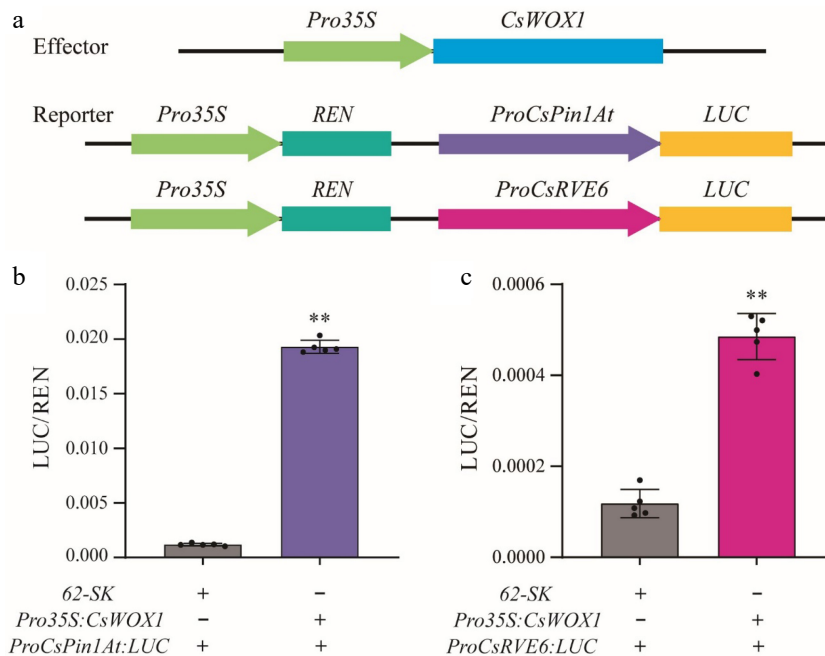


**Fig. 7** CsWOX1 activates the expression of *CsRVE6* and *CsPin1At*. (a) Structural diagram of the reporter and effector constructs used for LUC/REN assays. LUC activity measurement after transient expression of *35S:CsWOX1* with (b) *ProCsPin1At:LUC* and (c) *ProCsRVE6:LUC* in tobacco leaves. The LUC/REN ratio from the empty vector (62-SK) combined with *ProCsPin1At:LUC* and *ProCsRVE6:LUC* were used as the calibration. Two-tailed Student's t-test was performed and statistically significant differences were indicated by \*\*  $p < 0.01$ . Values are mean  $\pm$  SD (n = 5).

Conversely, when the *CsWOX1* gene was mutated, both *GI* and *FKF1* genes down-regulated in this pathway. However, the expression levels of other genes in this pathway did not show significant differences, possibly due to the upregulation of the *LHY* homolog gene, *RVE8*, in the mutant. *RVE8* establishes a feedback loop with the *PRRs* family genes, thereby activating the expression of *PRR7* and *PRR9*, which in turn inhibit *CDF1*. This intricate network ensures that the expression of *CO* and *FT* in the mutant remains largely unaltered.

However, research on the association between *WOX* family genes and plant circadian rhythms is limited. When the homologous gene of Loquat, *EjWUSa*, is overexpressed in *Arabidopsis*, it exhibits early bolting by 10 d and precocious flowering by 9 d compared to the wild type, suggesting that *EjWUSa* can promote flowering in *Arabidopsis*<sup>[65]</sup>. Although the specific mechanisms by which the *CsWOX1* gene interacts with genes involved in plant circadian regulation and how it influences cucumber circadian regulation remained unknown, the present transcriptomic data and analysis has identified a significant number of differentially expressed genes related to plant rhythms. These findings lead us to propose that *CsWOX1* likely exerts some degree of influence on the plant's circadian clock, thereby laying the groundwork for further investigations into this area.

## Author contributions

The authors confirm contribution to the paper as follows: study conception and design: Li Z, Shen J, Zhang A, Jiang Y; data collection: Zhang A, Li X, Zhang H; analysis and interpretation of results: Zhang A, Li X, Zhang H, Jiang Y, Li Q; draft manuscript preparation: Zhang A, Zhang H, Li X, Jiang Y, Li Q. All authors reviewed the results and approved the final version of the manuscript.

## Data availability

The data that support the findings of this study are available in the NCBI repository. These data were derived from the following

resources available in the public domain: [www.ncbi.nlm.nih.gov/bioproject/PRJNA1138173](http://www.ncbi.nlm.nih.gov/bioproject/PRJNA1138173).

## Acknowledgments

This research was funded by the National Key Research and Development Program of China (2022 YFD1602000), the National Natural Science Foundation of China (32202519, U22A20498), the Science and Technology Innovation Team of Shaanxi (2021TD-32), and the Key Research and Development Program of Shaanxi (S2023-YF-YBNY-0530). The authors would like to thank Dr. Hu Wang for providing valuable transcriptomic data. Thank you to all those who made this research possible.

## Conflict of interest

The authors declare that they have no conflict of interest.

**Supplementary information** accompanies this paper at (<https://www.maxapress.com/article/doi/10.48130/vegres-0024-0038>)

## Dates

Received 28 August 2024; Revised 19 October 2024; Accepted 28 October 2024; Published online 11 February 2025

## References

- Barton MK. 2010. Twenty years on: the inner workings of the shoot apical meristem, a developmental dynamo. *Developmental Biology* 341:95–113
- Du F, Guan C, Jiao Y. 2018. Molecular mechanisms of leaf morphogenesis. *Molecular Plant* 11:1117–34
- Donnelly PM, Bonetta D, Tsukaya H, Dengler RE, Dengler NG. 1999. Cell cycling and cell enlargement in developing leaves of *Arabidopsis*. *Developmental Biology* 215:407–19

4. Ichihashi Y, Kawade K, Usami T, Horiguchi G, Takahashi T, et al. 2011. Key proliferative activity in the junction between the leaf blade and leaf petiole of *Arabidopsis*. *Plant Physiology* 157:1151–62
5. Caggiano MP, Yu X, Bhatia N, Larsson A, Ram H, et al. 2017. Cell type boundaries organize plant development. *eLife* 6:e27421
6. Yu T, Guan C, Wang J, Sajjad M, Ma L, et al. 2017. Dynamic patterns of gene expression during leaf initiation. *Journal of Genetics and Genomics* 44:599–601
7. Emery JF, Floyd SK, Alvarez J, Eshed Y, Hawker NP, et al. 2003. Radial patterning of *Arabidopsis* shoots by class IIIHD-ZIP and KANADI genes. *Current Biology* 13:1768–74
8. McConnell JR, Emery J, Eshed Y, Bao N, Bowman J, et al. 2001. Role of *PHABULOSA* and *PHAVOLUTA* in determining radial patterning in shoots. *Nature* 411:709–13
9. Shen J, Jiang Y, Pan J, Sun L, Li Q, et al. 2024. The GRAS transcription factor CsTL regulates tendril formation in cucumber. *The Plant Cell* 36:2818–33
10. Jiang Y, Zhang A, He W, Li Q, Zhao B, et al. 2023. GRAS family member LATERAL SUPPRESSOR regulates the initiation and morphogenesis of watermelon lateral organs. *Plant Physiology* 193:2592–604
11. Iwakawa H, Ueno Y, Semiarti E, Onouchi H, Kojima S, et al. 2002. The *ASYMMETRIC LEAVES2* gene of *Arabidopsis thaliana*, required for formation of a symmetric flat leaf lamina, encodes a member of a novel family of proteins characterized by cysteine repeats and a leucine zipper. *Plant and Cell Physiology* 43:467–78
12. Lin WC, Shuai B, Springer PS. 2003. The *Arabidopsis* LATERAL ORGAN BOUNDARIES-domain gene *ASYMMETRIC LEAVES2* functions in the repression of *KNOX* gene expression and in adaxial-abaxial patterning. *The Plant Cell* 15:2241–52
13. Xu Y, Sun Y, Liang W, Huang H. 2002. The *Arabidopsis* AS2 gene encoding a predicted leucine-zipper protein is required for the leaf polarity formation. *Acta Botanica Sinica* 44:1194–202
14. Kerstetter RA, Bollman K, Taylor RA, Bomblies K, Poethig RS. 2001. *KANADI* regulates organ polarity in *Arabidopsis*. *Nature* 411:706–09
15. Gray JA, Shalit-Kaneh A, Chu DN, Hsu PY, Harmer SL. 2017. The *REVEILLE* clock genes inhibit growth of juvenile and adult plants by control of cell size. *Plant Physiology* 173:2308–22
16. Hsu PY, Devisetty UK, Harmer SL. 2013. Accurate timekeeping is controlled by a cycling activator in *Arabidopsis*. *eLife* 2:e00473
17. Xi W, Gong X, Yang Q, Yu H, Liou YC. 2016. Pin1At regulates PIN1 polar localization and root gravitropism. *Nature Communications* 7:10430
18. Lee H, Suh SS, Park E, Cho E, Ahn JH, et al. 2000. The AGAMOUS-LIKE 20 MADS domain protein integrates floral inductive pathways in *Arabidopsis*. *Genes & Development* 14:2366–76
19. Liu C, Chen H, Er HL, Soo HM, Kumar PP, et al. 2008. Direct interaction of *AGL24* and *SOC1* integrates flowering signals in *Arabidopsis*. *Development* 135:1481–91
20. Wang Y, Liu C, Yang D, Yu H, Liou YC. 2010. Pin1At Encoding a peptidyl-prolyl *cis/trans* isomerase regulates flowering time in *Arabidopsis*. *Molecular Cell* 37:112–22
21. Haecker A, Groß-Hardt R, Geiges B, Sarkar A, Breuninger H, et al. 2004. Expression dynamics of *WOX* genes mark cell fate decisions during early embryonic patterning in *Arabidopsis thaliana*. *Development* 131:657–68
22. Laux T, Mayer KFX, Berger J, Jürgens G. 1996. The *WUSCHEL* gene is required for shoot and floral meristem integrity in *Arabidopsis*. *Development* 122:87–96
23. Nakata M, Matsumoto N, Tsugeki R, Rikirsch E, Laux T, et al. 2012. Roles of the middle domain-specific *WUSCHEL-RELATED HOMEBOX* genes in early development of leaves in *Arabidopsis*. *The Plant Cell* 24:519–35
24. Zhang Z, Runions A, Mentink RA, Kierzkowski D, Karady M, et al. 2020. A *WOX/auxin* biosynthesis module controls growth to shape leaf form. *Current Biology* 30:4857–4868.E6
25. Vandenbussche M, Horstman A, Zethof J, Koes R, Rijpkema AS, et al. 2009. Differential recruitment of *WOX* transcription factors for lateral development and organ fusion in *Petunia* and *Arabidopsis*. *The Plant Cell* 21:2269–83
26. Lin H, Niu L, McHale NA, Ohme-Takagi M, Mysore KS, et al. 2013. Evolutionarily conserved repressive activity of *WOX* proteins mediates leaf blade outgrowth and floral organ development in plants. *Proceedings of the National Academy of Sciences of the United States of America* 110:366–71
27. McHale NA, Marcotrigiano M. 1998. *LAM1* is required for dorsoventrality and lateral growth of the leaf blade in *Nicotiana*. *Development* 125:4235–43
28. Tadege M, Lin H, Bedair M, Berbel A, Wen J, et al. 2011. *STENOFOLIA* regulates blade outgrowth and leaf vascular patterning in *Medicago truncatula* and *Nicotiana sylvestris*. *The Plant Cell* 23:2125–42
29. Zhuang LL, Ambrose M, Rameau C, Weng L, Yang J, et al. 2012. *LATHYROIDES*, encoding a *WUSCHEL*-related homeobox1 transcription factor, controls organ lateral growth, and regulates tendril and dorsal petal identities in garden pea (*Pisum sativum* L.). *Molecular Plant* 5:1333–45
30. Wang C, Zhao B, He L, Zhou S, Liu Y, et al. 2021. The *WOX* family transcriptional regulator *SILAM1* controls compound leaf and floral organ development in *Solanum lycopersicum*. *Journal of Experimental Botany* 72:1822–35
31. Niu L, Lin H, Zhang F, Watira TW, Li G, et al. 2015. *LOOSE FLOWER*, a *WUSCHEL*-like Homeobox gene, is required for lateral fusion of floral organs in *Medicago truncatula*. *The Plant Journal* 81:480–92
32. Vandenbussche M. 2021. The role of *WOX1* genes in blade development and beyond. *Journal of Experimental Botany* 72:1514–16
33. Ishiwata A, Ozawa M, Nagasaki H, Kato M, Noda Y, et al. 2013. Two *WUSCHEL*-related homeobox genes, *narrow leaf2* and *narrow leaf3*, control leaf width in rice. *Plant and Cell Physiology* 54:779–92
34. Nardmann J, Ji J, Werr W, Scanlon MJ. 2004. The maize duplicate genes *narrow sheath1* and *narrow sheath2* encode a conserved homeobox gene function in a lateral domain of shoot apical meristems. *Development* 131:2827–39
35. Scanlon MJ, Schneeberger RG, Freeling M. 1996. The maize mutant *narrow sheath* fails to establish leaf margin identity in a merostematic domain. *Development* 122:1683–91
36. Niu H, Liu X, Tong C, Wang H, Li S, et al. 2018. The *WUSCHEL*-related homeobox1 gene of cucumber regulates reproductive organ development. *Journal of Experimental Botany* 69:5373–87
37. Wang H, Niu H, Li C, Shen G, Liu X, et al. 2020. *WUSCHEL*-related homeobox1 (*WOX1*) regulates vein patterning and leaf size in *Cucumis sativus*. *Horticulture Research* 7:182
38. Wang HS, Yu C, Fan PP, Bao BF, Li T, et al. 2015. Identification of two cucumber putative silicon transporter genes in *Cucumis sativus*. *Journal of Plant Growth Regulation* 34:332–38
39. Livak KJ, Schmittgen TD. 2001. Analysis of relative gene expression data using real-time quantitative PCR and the  $2^{-\Delta\Delta CT}$  method. *Methods* 25:402–08
40. Hellens RP, Allan AC, Friel EN, Bolitho K, Grafton K, et al. 2005. Transient expression vectors for functional genomics, quantification of promoter activity and RNA silencing in plants. *Plant Methods* 1:13
41. Zhang Y, Wu R, Qin G, Chen Z, Gu H, et al. 2011. Over-expression of *WOX1* leads to defects in meristem development and polyamine homeostasis in *Arabidopsis*. *Journal of Integrative Plant Biology* 53:493–506
42. Titapiwatanakun B, Blakeslee JJ, Bandyopadhyay A, Yang H, Mravec J, et al. 2009. *ABC19/PGP19* stabilises *PIN1* in membrane microdomains in *Arabidopsis*. *The Plant Journal* 57:27–44
43. Verrier PJ, Bird D, Buria B, Dassa E, Forestier C, et al. 2008. Plant ABC proteins – a unified nomenclature and updated inventory. *Trends in Plant Science* 13:151–59
44. Mishra P, Panigrahi KC. 2015. *GIGANTEA* – an emerging story. *Frontiers in Plant Science* 6:8
45. Yan J, Li X, Zeng B, Zhong M, Yang J, et al. 2020. *FKF1* F-box protein promotes flowering in part by negatively regulating *DELLA* protein stability under long-day photoperiod in *Arabidopsis*. *Journal of Integrative Plant Biology* 62:1717–40
46. Kamimoto Y, Terasaka K, Hamamoto M, Takanashi K, Fukuda S, et al. 2012. *Arabidopsis* *ABC21* is a facultative auxin importer/exporter regulated by cytoplasmic auxin concentration. *Plant and Cell Physiology* 53:2090–100
47. Jenness MK, Carraro N, Pritchard CA, Murphy AS. 2019. The *Arabidopsis* ATP-BINDING CASSETTE transporter *ABC21* regulates auxin levels in cotyledons, the root pericycle, and leaves. *Frontiers in Plant Science* 10:806

48. Noh B, Murphy AS, Spalding EP. 2001. *Multidrug resistance*-like genes of *Arabidopsis* required for auxin transport and auxin-mediated development. *The Plant Cell* 13:2441–54
49. Geisler M, Kolukisaoglu HÜ, Bouchard R, Billion K, Berger J, et al. 2003. TWISTED DWARF1, a unique plasma membrane-anchored immunophilin-like protein, interacts with *Arabidopsis* multidrug resistance-like transporters AtPGP1 and AtPGP19. *Molecular Biology of the Cell* 14:4238–49
50. Farinas B, Mas P. 2011. Functional implication of the MYB transcription factor RVE8/LCL5 in the circadian control of histone acetylation. *The Plant Journal* 66:318–29
51. Rawat R, Takahashi N, Hsu PY, Jones MA, Schwartz J, et al. 2011. REVEILLE8 and PSEUDO-RESPONSE REGULATOR5 form a negative feedback loop within the *Arabidopsis* circadian clock. *PLoS Genetics* 7:e1001350
52. Schaffer R, Ramsay N, Samach A, Corden S, Putterill J, et al. 1998. The *late elongated hypocotyl* mutation of *Arabidopsis* disrupts circadian rhythms and the photoperiodic control of flowering. *Cell* 93:1219–29
53. Wang ZY, Tobin EM. 1998. Constitutive expression of the *CIRCADIAN CLOCK ASSOCIATED 1* (CCA1) gene disrupts circadian rhythms and suppresses its own expression. *Cell* 93:1207–17
54. Alabadí D, Yanovsky MJ, Más P, Harmer SL, Kay SA. 2002. Critical role for CCA1 and LHY in maintaining circadian rhythmicity in *Arabidopsis*. *Current Biology* 12:757–61
55. Nagel DH, Doherty CJ, Pruneda-Paz JL, Schmitz RJ, Ecker JR, et al. 2015. Genome-wide identification of CCA1 targets uncovers an expanded clock network in *Arabidopsis*. *Proceedings of the National Academy of Sciences of the United States of America* 112:E4802–E4810
56. Gendron JM, Pruneda-Paz JL, Doherty CJ, Gross AM, Kang SE, et al. 2012. *Arabidopsis* circadian clock protein, TOC1, is a DNA-binding transcription factor. *Proceedings of the National Academy of Sciences of the United States of America* 109:3167–72
57. Kamioka M, Takao S, Suzuki T, Taki K, Higashiyama T, et al. 2016. Direct repression of evening genes by CIRCADIAN CLOCK-ASSOCIATED1 in the *Arabidopsis* circadian clock. *The Plant Cell* 28:696–711
58. Pokhilko A, Fernández AP, Edwards KD, Southern MM, Halliday KJ, et al. 2012. The clock gene circuit in *Arabidopsis* includes a repressilator with additional feedback loops. *Molecular Systems Biology* 8:574
59. Scandola S, Mehta D, Li Q, Gallo MCR, Castillo B, et al. 2022. Multi-omic analysis shows REVEILLE clock genes are involved in carbohydrate metabolism and proteasome function. *Plant Physiology* 190:1005–23
60. Song YH, Ito S, Imaizumi T. 2013. Flowering time regulation: photoperiod- and temperature-sensing in leaves. *Trends in Plant Science* 18:575–83
61. Amasino R. 2010. Seasonal and developmental timing of flowering. *The Plant Journal* 61:1001–13
62. Samach A, Onouchi H, Gold SE, Ditta GS, Schwarz-Sommer Z, et al. 2000. Distinct roles of CONSTANS target genes in reproductive development of *Arabidopsis*. *Science* 288:1613–16
63. Imaizumi T, Schultz TF, Harmon FG, Ho LA, Kay SA. 2005. FKF1 F-BOX protein mediates cyclic degradation of a repressor of CONSTANS in *Arabidopsis*. *Science* 309:293–97
64. Sawa M, Nusinow DA, Kay SA, Imaizumi T. 2007. FKF1 and GIGANTEA complex formation is required for day-length measurement in *Arabidopsis*. *Science* 318:261–65
65. Yu Y, Yang M, Liu X, Xia Y, Hu R, et al. 2022. Genome-wide analysis of the WOX gene family and the role of *EjWUSa* in regulating flowering in loquat (*Eriobotrya japonica*). *Frontiers in Plant Science* 13:1024515



Copyright: © 2025 by the author(s). Published by Maximum Academic Press, Fayetteville, GA. This article is an open access article distributed under Creative Commons Attribution License (CC BY 4.0), visit <https://creativecommons.org/licenses/by/4.0/>.